Bioorganic & Medicinal Chemistry 20 (2012) 3065–3071

Contents lists available at SciVerse ScienceDirect

Bioorganic & Medicinal Chemistry

journal homepage: www.elsevier.com/locate/bmc

Synthesis and evaluation of [^{18}F]fluororasagiline, a novel positron emission tomography (PET) radioligand for monoamine oxidase B (MAO-B)

S. Nag [a,*], L. Lehmann [b], G. Kettschau [b], T. Heinrich [b], A. Thiele [b], A. Varrone [a], B. Gulyas [a], C. Halldin [a]

[a] Karolinska Institutet, Department of Clinical Neuroscience, Psychiatry Section, Karolinska Hospital, S-17176 Stockholm, Sweden
[b] Bayer HealthCare AG, Global Drug Discovery, Berlin, Germany

ARTICLE INFO

Article history:
Received 7 December 2011
Revised 23 February 2012
Accepted 25 February 2012
Available online 3 March 2012

Keywords:
Monoamine oxidase
PET
Autoradiography
Fluorine-18
Biodistribution
Kinetics
Metabolites and non-human primate

ABSTRACT

The aim of this study was to synthesize and evaluate a novel fluorine-18 labeled analogue of rasagiline (**6**) as a PET radioligand for monoamine oxidase B (MAO-B). The corresponding non-radioactive fluorine-19 ligand, (1*S*,2*S*)-2-fluoro-*N*-(prop-2-yn-1-yl)indan-1-amine (**4**), was characterized in in vitro assays.

The precursor compound (3a*S*,8a*R*)-3-(prop-2-yn-1-yl)-3,3a,8,8a-tetrahydroindeno[1,2-*d*][1,2,3]oxathiazole 2,2-dioxide (**3**) and reference standard **4** were synthesized in multi-step syntheses. Recombinant human MAO-B and MAO-A enzyme preparations were used in order to determine IC_{50} values for compound **4** by use of an enzymatic assay employing kynuramine as substrate. Radiolabeling was accomplished by a two-step synthesis, compromising a nucleophilic substitution followed by hydrolysis of the sulphamidate group. Human whole hemisphere autoradiography (ARG) was performed with [^{18}F]fluororasagiline. Blocking experiments with pirlindole (MAO-A), L-deprenyl and rasagiline (MAO-B) were conducted to demonstrate the specificity of the binding. A positron emission tomography (PET) study was carried out in a cynomolgus monkey where time activity curves for whole brain and regions with high and low MAO-B activity were recorded. Radiometabolites were measured in monkey plasma using gradient HPLC.

Compound **4** inhibited MAO-B with an IC_{50} of 27 nM and MAO-A with an IC_{50} of 2.3 μM. Radiolabeling of precursor **3** and subsequent hydrolysis of the protecting group towards (1*S*,2*S*)-2-[^{18}F]fluoro-*N*-(prop-2-yn-1-yl)indan-1-amine (**6**) was successfully accomplished with an radiochemical yield of 40–70%, a radiochemical purity higher than 99% and a specific radioactivity higher than 200 GBq/μmol. ARG demonstrated selective binding for [^{18}F]fluororasagiline (**6**) to MAO-B containing brain regions, for example, striatum. The initial uptake in the monkey brain was 250% SUV at 4 min post injection. The highest amounts of radioactivity were observed in the striatum and thalamus as expected whereas in the cortex and cerebellum lower levels were observed. Metabolite studies demonstrated 30% unchanged radioligand at 90 min post injection.

Our investigations demonstrated that the new ligand [^{18}F]fluororasagiline (**6**) binds specifically to MAO-B in vitro and has a MAO-B specific binding pattern in vivo. Thus, it could serve as a novel potential candidate for human PET studies.

1. Introduction

Monoamine oxidases (MAOs) are important enzymes that metabolize biogenic amines in the periphery and the CNS.[1] MAO enzymes exist in two forms such as MAO-A and MAO-B.[2] MAO-B predominates over MAO-A in the primate and human brain and it metabolizes dopamine to the inactive compound dihydroxyphenylacetic acid which is further metabolized to homovanillic acid. Inhibition of MAO-B blocks the metabolism of dopamine, and thereby prolongs its activity.[3] Monoamine oxidase inhibitors (MAOIs) such as L-deprenyl, rasagiline, moclobemide have been used to treat psychiatric and neurological disorders for many years according to their specific type of action such as irreversible and reversible inhibition, respectively.[4]

Rasagiline is a highly selective, irreversible MAO-B inhibitor that has been developed as a treatment for Parkinson's disease (PD).[5] Chemically, rasagiline is a *N*-propargyl aminoindan and

Abbreviations: PET, positron emission tomography; MAO, monoamino oxidase; MAOI, monoamino oxidase inhibitor; PD, Parkinson's disease; AD, Alzheimer's disease; NMR, nuclear magnetic resonance; UPLC, ultra performance liquid chromatograpy; HPLC, high performance liquid chromatography; LC, liquid chromatography; LC–MS, liquid chromatography–mass spectrometry; DMSO, dimethylsuphoxide; DMF, dimethylformamide; PBS, phosphate buffered solution; IC, inhibitory concentration; SUV, standard uptake value; ROI, region of interest.

* Corresponding author. Tel.: +46 8 51775018.
E-mail address: sangram.nag@ki.se (S. Nag).

0968-0896/$ - see front matter © 2012 Elsevier Ltd. All rights reserved.
doi:10.1016/j.bmc.2012.02.056

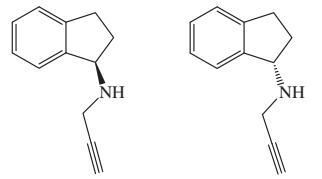

Figure 1. Structures of *R*(+)rasagiline (**1**) and *S*(−)rasagiline (**2**).

exists in two stereoisomers, namely *R*(+)rasagiline (*N*-propargyl-1*R*(+)aminoindan) and *S*(−)rasagiline (*N*-propargyl-1*S*(−)aminoindan) (Fig. 1). In terms of MAO-B inhibition the *R*-isomer exhibits 4 times higher potency over the *S*-isomer.[6]

Positron emission tomography (PET) has been applied as a useful tool for imaging brain MAO-B activity in humans for studying neurodegenerative diseases[7] and epilepsy.[8] Several radioligands have been developed in order to study MAO-B activity and density by PET such as [^{11}C]MD-230254, a reversible MAO-B inhibitor,[9] [^{11}C]pargyline,[10] [^{11}C]L-deprenyl,[11] [^{11}C]deuterium-L-deprenyl,[12] [^{11}C]SL25.1188,[13] DL-4-[^{18}F]fluorodeprenyl,[14] 6-[^{18}F]fluoro-*N*-methyl-*N*-(prop-2-yn-1-yl)hexan-1-amine[15] all behaving as irreversible MAO-B inhibitors. Among those radioligands [^{11}C]L-deprenyl is the one most widely used in clinical and preclinical studies. However, the short half life of carbon-11 (20.4 min) makes carbon-11 labeled tracers not suitable for distribution to PET centers not equipped with an on-site cyclotron. Another major drawback of [^{11}C]L-deprenyl is that its main radiometabolite [^{11}C]L-methamphetamine enters the brain. A multistep radiosynthesis and undesired radiometabolite preclude efficient use of DL-4-[^{18}F]fluorodeprenyl and 6-[^{18}F]fluoro-*N*-methyl-*N*-(prop-2-yn-1-yl)hexan-1-amine. There is a high interest in the development of labeled MAO-B inhibitors with longer half-life as biological probes to map MAO-B activity in brain. Recently, we have developed three novel fluorine-18 labeled analogues of L-deprenyl for PET studies of MAO-B.[16]

Both rasagiline and L-deprenyl possess propargyl groups, which are a prerequisite for their inhibitory activity on MAO-B. However, the molecules differ in their basic structures and metabolic products. Aminoindan, the metabolite of rasagiline (Fig. 2), is in contrast to the amphetamine-like metabolites of L-deprenyl not prone to bind to the dopamine transporter. Therefore, we used rasagiline as the chemical entity for the development of a novel MAO-B PET ligand.

In the present study our aims were (i) to develop a fast and efficient synthetic method for labeling of a novel fluororasagiline analogue with fluorine-18, (ii) to characterize its in vitro MAO-B and MAO-A inhibition based on the rate of kynuramine oxidation, (iii) to evaluate its binding to MAO-B in various brain structures in post mortem human brain slices using an autoradiography technique and (iv) to evaluate the in vivo characteristics of [^{18}F]fluororasagiline by PET measurement in a non-human primate in order to develop a suitable fluorine-18 labeled radioligand for examination of MAO-B activity in vivo by PET.

2. Results and discussion

2.1. Chemistry

The precursor compound (**3**) and the reference standard fluororasagiline (**4**) were synthesized from the starting aminoindanol (**1**) by multistep organic synthesis (Scheme 1). In the first step, (1*S*,2*R*)-1-aminoindan-2-ol (**1**) was treated with highly reactive sulfuryl chloride. The key parameter of this reaction was to keep the temperature at −65 °C. (3a*S*,8a*R*)-3,3a,8,8a-tetrahydroindeno[1,2-*d*][1,2,3]oxathiazole 2,2-dioxide (**2**) was synthesized with high yield (90%). In the second step, tetrahydroindeno[1,2-*d*][1,2,3]oxathiazole 2,2-dioxide was alkylated with propargyl bromide to give the precursor compound (**3**) in a moderate 68% isolated yield, following a previously reported method.[17] Reference standard fluororasagiline (**4**) was synthesised with inversion of configuration from (3a*S*,8a*R*)-3-[prop-2-yn-1-yl]-3,3a,8,8a-tetrahydroindeno[1,2-*d*][1,2,3]oxathiazole 2,2-dioxide (**3**) by two step synthesis. The first step was substitution reaction with caesium fluoride followed by hydrolysis of sulphamidate group with addition of 4*N* hydrochloric acid (15 mL) and ethanol. Several acids were tested for the hydrolysis of sulphamidate group and 5*N* HCl gave the best yield. A sample of the material was submitted to X-ray crystallography analysis confirming the assigned absolute stereochemistry. Both the precursor compound (**3**) and the reference standard (**4**) were found to be stable over several months and stored at 0 to −20 °C.

2.2. Radiochemistry

The radiolabeling was achieved by nucleophilic substitution of the sulphamidate precursors (**3**) by [^{18}F]fluoride in presence of $K_{2.2.2}$ and K_2CO_3 followed by deprotection of the sulphamidate group as shown in Scheme 2. Different acids such as sulfuric acid, trifluoroacetic acid, hydroiodic acid and hydrochloric acid were tested for the hydrolysis of the sulphamidate group. Trifluoroacetic acid and hydroiodic acid did not result any hydrolysed product. Whereas sulfuric acid gave the hydrolysed product with the mixture of other undesired radio labeled compounds. Hydrolysis with hydrochloric acid (200 μL of 0.5 N) gave the highest yield at 110 °C. The overall radiosynthesis including the fluorination reaction,

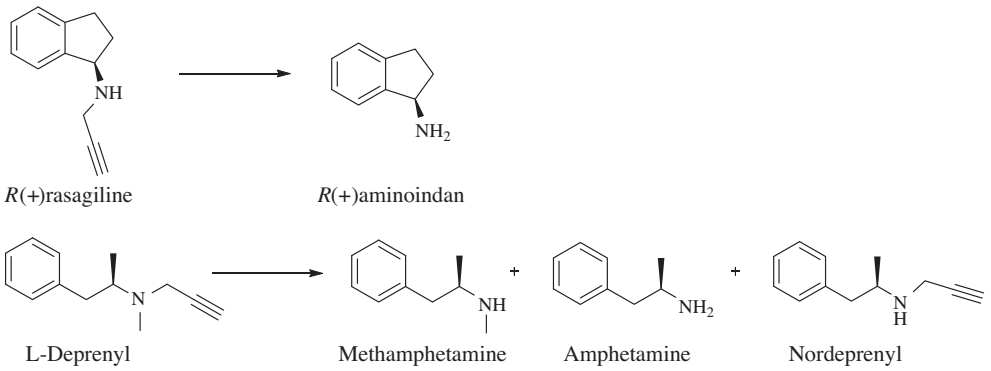

Figure 2. Proposed metabolism of rasagiline and L-deprenyl.

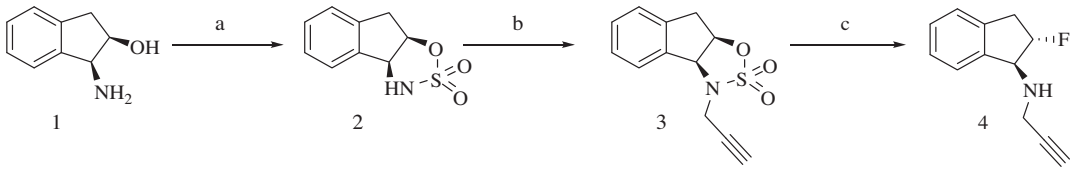

Scheme 1. Synthesis of precursor and reference standard for [^{18}F]fluororasagiline. Reagents and conditions: (a) SO_2Cl_2/triethylamine; (b) K_2CO_3/propargyl bromide; (c) CsF/5 N HCl.

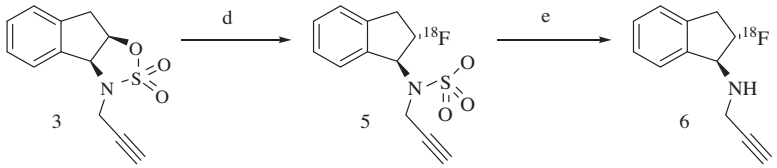

Scheme 2. Radiolabeling of [^{18}F]fluororasagiline. Reagents and conditions: (d) K^{18}F, K-2,2,2/DMSO; (e) 0.5 N HCl.

deprotection of the sulphamidate group, HPLC purification, SPE purification and radiotracer formulation was completed within 75–80 min.

The average radiochemical yield of the radiosynthesis was 55%, and the radiochemical purity was higher than 99% for [^{18}F]fluororasagiline. The identity of the labeled compound was confirmed by co-injection of their corresponding fluorine-19 analogue **4** using analytical HPLC. The radioligand [^{18}F]fluororasagiline was found to be stable (>97%) in PBS buffered solution (pH 7.4) for the duration of 180 min at room temperature.

2.3. In vitro inhibition of MAO-A and MAO-B

The concentration of the fluorine-19 analogue of rasagiline that is necessary to inhibit the enzymatic activities of MAO-B and MAO-A, respectively, was determined based on the rate of 4-OH-quinoline generation from kynuramine. The compound inhibited MAO-B with an IC_{50} = 27.0 ± 2.0 nM while it was inhibiting MAO-A with an IC_{50} = 2.3 ± 0.08 μM. L-Deprenyl and rasagiline were used as reference compounds in the assay. L-deprenyl and rasagiline inhibited MAO-B with an IC_{50} of 13 ± 0.4 and 46.0 ± 2.2 nM, respectively. Thus, compound **4** inhibited MAO-B in a range comparable to that of the therapeutically used compounds L-deprenyl and rasagiline. Compound **4** was ca. 84 times more potent in inhibiting MAO-B versus MAO-A hinting to its specificity.

2.4. Autoradiography

The total binding pattern of [^{18}F]fluororasagiline, that is, binding comprising specific and non-specific binding, are displayed in whole hemisphere brain slices obtained from control subjects (Fig. 3). The signal intensities were highest in the hippocampus, the putamen, the caudate nucleus, the external globus pallidus and the thalamus. For blocking the MAO-A ligand pirlindole and the MAO-B ligands L-deprenyl and rasagiline have been used in 10 μM concentrations (Fig. 3). The MAO-B ligands rasagiline and L-deprenyl completely blocked the binding of [^{18}F]fluororasagiline, whereas the MAO-A ligand pirlindole did not block the binding.

These observations indicate that [^{18}F]fluororasagiline is a selective radioligand of MAO-B , displaying no binding to the MAO-A isoform.

2.5. PET measurements in a cynomolgus monkey

The radioactive uptake of [^{18}F]fluororasagiline in a cynomolgus monkey brain is shown in Figure 4. [^{18}F]Fluororasagiline readily

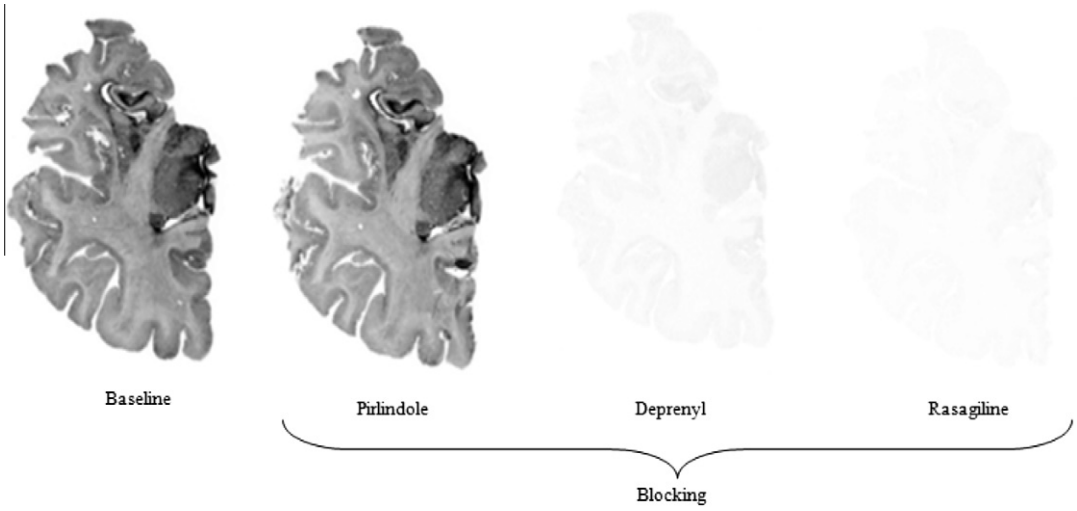

Figure 3. Coronal slices of human brain autoradiograms labeled with [^{18}F]fluororasagiline at baseline conditions and during incubation with pirlindole (10 μM), L-deprenyl (10 μM) and rasagiline (10 μM).

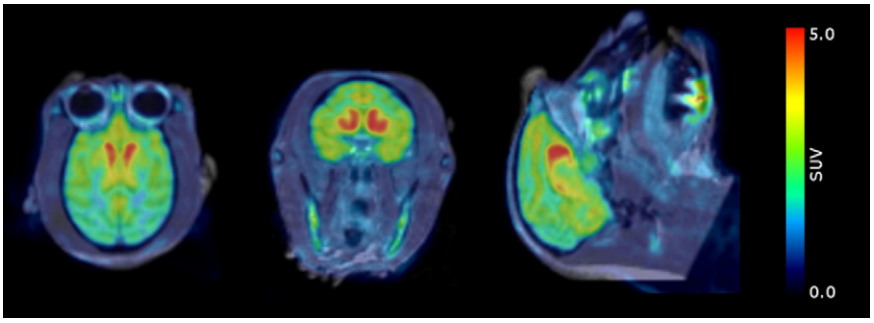

Figure 4. PET images of [^{18}F]fluororasagiline co-registered with MRI and averaged between 9 and 120 min in the horizontal (left), sagittal (middle) and coronal (right) projections.

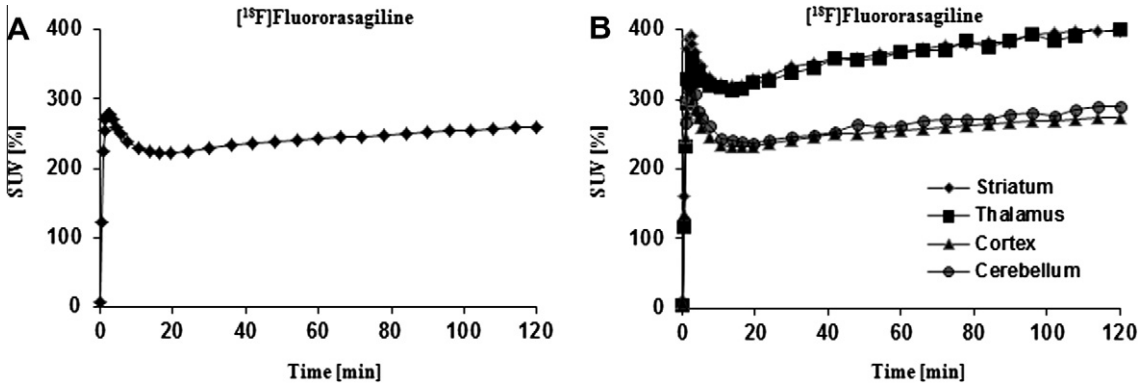

Figure 5. Brain uptake expressed as percent standardised uptake value (%SUV). (A) Time activity curves after iv injection of [^{18}F]fluororasagiline in whole brain, (B) time activity curves of [^{18}F]fluororasagiline in different brain regions.

crossed the blood–brain barrier and bound rapidly to its target sites. The brain uptake in a baseline condition was high (250% SUV at 4 min p.i) (Fig. 5A). Due to the irreversible binding kinetics, [^{18}F]fluororasagiline did not show any wash-out from the brain. The uptake of [^{18}F]fluororasagiline at baseline conditions was highest in the striatum and thalamus and lowest in the cerebellum and in cortical areas (Fig. 5B), consistent with the known distribution of in vivo MAO-B activity as previously reported for [^{11}C]deprenyl.[11]

Despite the promising brain uptake, the experiment revealed one potential problem with [^{18}F]fluororasagiline, namely that the radioactivity continued increasing slowly throughout the PET measurement. This finding may be explained by brain penetration of the radiometabolites such as [^{18}F]a and/or [^{18}F]b.

2.6. Metabolite analysis

The recovery of radioactivity from plasma into acetonitrile after deproteinization was higher than 95%. HPLC analysis of plasma following injection of [^{18}F]fluororasagiline, which eluted at 7.7 min, revealed the presence of three more major peaks, [^{18}F]a, [^{18}F]fluoroaminoindan and [^{18}F]b with retention times of 2.7, 4.6 and 9.2 min, respectively (Fig. 6A). The parent compound was more abundant at 45 min representing approximately 50% of the plasma

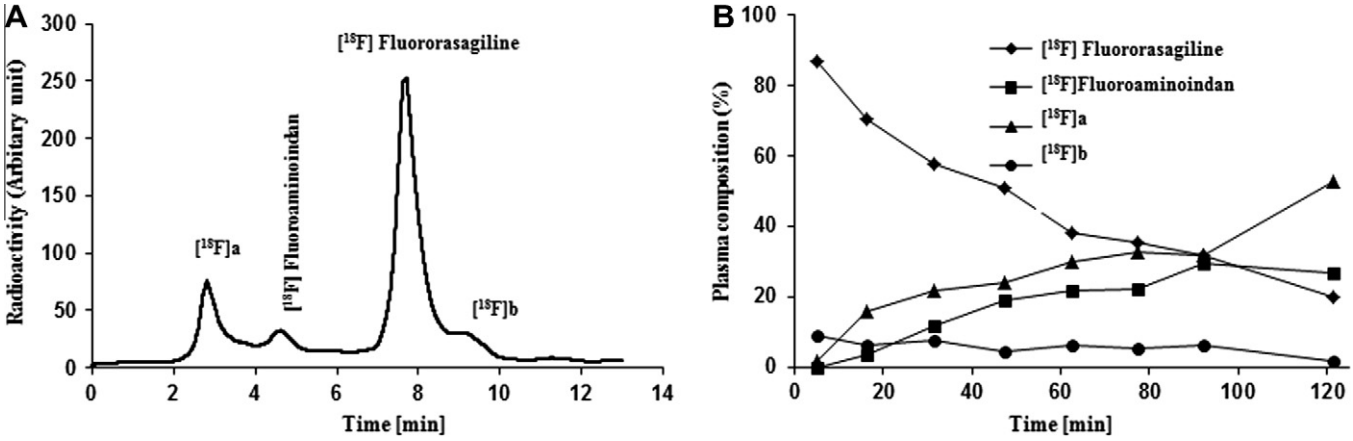

Figure 6. Metabolite analysis during the course of the PET measurements. (A) A representative HPLC chromatogram 15 min after injection of [^{18}F]fluororasagiline showing the retention times of the metabolites and the parent compound, (B) the in vivo metabolism of [^{18}F]fluororasagiline is shown as the relative plasma composition of metabolites and parent compound in % of total plasma radioactivity that was injected.

radioactivity and it decreased to 20% at 120 min (Fig. 6B). The identity of the radiometabolite [^{18}F]fluoroaminoindan was confirmed by co-injection with the authentic non-radioactive fluoroaminoindan and the radiometabolites [^{18}F]a and [^{18}F]b were not further analysed for identification.

3. Conclusion

The present study demonstrated that the radioligand [^{18}F]fluororasagiline was efficiently labeled with fluorine-18 and has nano-molar in vitro binding affinity to recombinant MAO-B (IC_{50} = 27 nM) with ca. 84 times lower affinity to MAO-A (IC_{50} = 2.3 μM). In post-mortem human brain autoradiography [^{18}F]fluororasagiline exhibited high specificity to MAO-B. A PET measurement in a cynomolgus monkey showed a high brain uptake in known MAO-B rich regions. However, a continuing increase of the radioactivity throughout the PET scan may indicate a blood–brain barrier penetrating radiometabolite that may in turn complicate a reliable quantification. It is considered to synthesize a deuterated analogue of [^{18}F]fluororasagiline in order to investigate whether this leads to a reduced production of radiometabolites and will improve the kinetics of the tracer in the brain.

4. Materials and methods

4.1. Chemistry

NMR spectra were recorded on Varian Unity-400 and Bruker Avance 400 (^{1}H, 400 MHz and ^{13}C, 100 MHz), and Bruker Avance 600 III (^{1}H, 600 MHz) NMR instruments. ^{1}H NMR spectra were referenced internally on $CDCl_3$ (δ^1H 7.26) and ^{13}C NMR spectra were referenced internally on $CDCl_3$ (δ^{13}C 77.20). For the purification of [^{18}F]fluororasagiline high performance liquid chromatography (HPLC) was performed with a Merck–Hitachi gradient pump and a Merck–Hitachi, L-4000 variable wavelength UV-detector. A μ-Bondapak C-18 column (300 × 7.8 mm, 10 μm; Waters instruments) was used with a flow of 3 mL/min. Specific radioactivity (SA), quality control and plasma analysis were determined by analytical HPLC using a μ-Bondapak reverse phase HPLC column (C18, 3.9 × 300 mm, 10 μm, Waters) with mobile phase CH_3CN/10 mM H_3PO_4 (15/85) and flow rate of 2 mL/min. LC-MS was performed using a Waters Quattra-Tof Premier micro mass spectrometer, or Waters SQD 3001 single quadrupole mass spectrometer, coupled to Waters Acquity UPLC instruments. The ionization mode used was electro spray positive ionization (ESI^+). Analytical TLC was carried out on 0.25 mm silica gel plates. All solvents and chemicals were obtained from commercial sources and used without further purification.

4.2. Synthesis of (3a*S*,8a*R*)-3,3a,8,8a-tetrahydroindeno[1,2-*d*]-[1,2,3]oxathiazole 2,2-dioxide (2)

To a solution of commercially available (−)-(1*S*,2*R*)-*cis*-1-aminoindan-2-ol (**1**) (12.8 g, 86 mmol) in dichloromethane (200 mL) triethylamine (29.9 mL, 214 mmol) was added, and the resulting mixture was cooled to −65 °C by means of acetone/dry ice. A solution of sulfuryl chloride (8.27 mL, 103 mmol) in dichloromethane (250 mL) was added slowly (approx. 1 drop/s) whilst maintaining temperature at −65 °C. Upon complete addition, the cooling bath was removed and the mixture was allowed to warm up to room temperature. Stirring at room temperature was continued for 24 h. The mixture was washed twice with 2 N hydrochloric acid (200 mL each); the combined aqueous layers were extracted with dichloromethane (200 mL). The combined organic layers were dried over sodium sulfate and evaporated. The crude residue was purified by column chromatography on silica gel (EtOAc in hexane 0%→100%), followed by trituration in hexane, gave an approx. 90% pure product (5.6 g, 28% yield). Repeated chromatography as described yielded a highly pure product.^{1}H NMR (300 MHz, DMSO-d_6) δ ppm 3.14 (d, 1H), 3.37 (dd, 1H), 5.29 (t, 1H), 5.52 (td, 1H), 7.14–7.44 (m, 4H), 8.32 (d, 1H).

MS (ESI): $[M-H]^-$ = 210.

4.3. Synthesis of (3a*S*,8a*R*)-3-[prop-2-yn-1-yl]-3,3a,8,8a-tetrahydroindeno[1,2-*d*][1,2,3]oxathiazole 2,2-dioxide (3)

To a solution of **2** (111.0 mg, 0.525 mmol) in dry THF (2 mL) potassium carbonate (300.0 mg, 2.17 mmol) was added and stirred at room temperature for 30 min. To the stirred solution propargyl bromide (98.8 mg, 0.788 mmol) was added dropwise and the reaction mixture was stirred for overnight at the same temperature, diluted with water (50 mL) and extracted with CH_2Cl_2 (3 × 50 mL). The organic phase was separated and washed with saturated $NaHCO_3$ solution (100 mL) and brine (100 mL) and dried over $MgSO_4$ and filtered. The solvent was removed under reduced pressure to obtain the crude product as light yellow oil. The crude product was purified by silica-gel column chromatography (hexane/ether 70:30) and resulted in the final product (90.0 mg, 0.36 mmol, 68% yield) as light yellow oil. The product was analyzed by NMR, HPLC and LC–MS. ^{1}H NMR (400 MHz, $CDCl_3$) δ ppm 2.53 (t, 1H), 3.47 (d, 2H), 4.04 (dd, *J* = 2.53 Hz, 1H), 4.19 (dd, 1H), 5.22–5.32 (m, 1H), 5.55 (dd, 6.82 Hz, 1H), 7.28–7.40 (m, 3H) and 7.48 (d, 1H). ^{13}C NMR (101 MHz, $CDCl_3$) δ ppm 37.16, 37.98, 66.31, 75.25, 76.40, 82.73, 125.56, 128.04, 130.15, 137.06 and 139.58.

MS (ESI): $[M+H]^+$ = 250.

4.4. (1*S*,2*S*)-2-fluoro-*N*-(prop-2-yn-1-yl)-indan-1-amine (4)

To a solution of **3** (600 mg, 2.41 mmol) in a mixture of DMF (2.0 mL) and *tert*-butanol (20 mL) caesium fluoride (439 mg, 2.89 mmol) was added, and the resulting mixture was stirred at room temperature for 3 days. To drive the reaction to completion, another portion of caesium fluoride (840 mg, 5.53 mmol) was added and the mixture was stirred for another 2 h at room temperature. An aliquot was evaporated (1/4; the remaining mixture was used for optimization experiments), re-dissolved in ethanol (2 mL) and 4*N* aqueous HCl (2 mL) and heated under reflux for 2.5 h. The resulting mixture was allowed to cool to room temperature, and then partitioned between ethyl acetate and saturated aqueous sodium carbonate. The aqueous layer was extracted with ethyl acetate and the combined organic layers were washed with brine, dried over sodium sulfate, and carefully evaporated (product is somewhat volatile). The residue was purified by column chromatography on silica gel (EtOAc in hexane 6%→60%) to give the desired product (52 mg, 46% aliquotation adjusted yield). The product was characterized by HNMR, FNMR, and CI-MS.

^{1}H NMR (400 MHz, $CDCl_3$) δ ppm 2.31 (t, *J* = 2.38 Hz, 1H), 3.09 (ddd, *J* = 24.6, 17.1, 3.26 Hz, 1H), 3.42 (ddd, *J* = 23.6, 16.8, 6.02 Hz, 1H), 3.53–3.66 (m, 2H), 4.51 (dd, *J* = 18.1, 2.76 Hz, 1H); 5.18 (ddt, *J* = 52.0, 6.30, 3.00 Hz, 1H), 7.21–7.39 (m, 4H).

^{19}F NMR (376 MHz, $CDCl_3$) δ ppm −180.23 (dtd, *J* = 52.8, 24.0, 18.4 Hz).

MS (CI): $[M+H]^+$ = 190.

4.5. Radiosynthesis of [^{18}F]fluororasagiline (6)

Fluorine-18 fluoride ([^{18}F]F^-)was produced from a GEMS PET trace Cyclotron using 16.4 MeV protons via the ^{18}O(p,n)^{18}F reaction on ^{18}O enriched water ([^{18}O]H_2O) and [^{18}F]F^- was isolated from [^{18}O]H_2O on a preconditioned SepPak QMA light anion exchange cartridge and subsequently eluted from the cartridge with a

solution of K_2CO_3 (1.8 mg, 13 μmol), Kryptofix 2.2.2 (4,7,13,16,21, 24-hexaoxa-1,10-diazabicyclo-[8.8.8]hexacosane-$K_{2.2.2}$) (9.8 mg, 26 μmol) in water (85 μL, 18 MΩ) and MeCN (2 mL) to a reaction vessel (10 mL).The solvents were evaporated at 160 °C for 10–15 min under continuous nitrogen flow (70 mL/min) to form a dry complex of $[^{18}F]F^-/K_2CO_3$/K2.2.2 and the residue was cooled to room temperature (RT).

The precursor (**3**) (~0.02 mmol, ~5 mg) in DMSO (500 μL) was added to the dry complex of $[^{18}F]F^-/K_2CO_3$/K2.2.2. The closed reaction vessel was heated at 130 °C for 20 min and cooled down to room temperature. HCl (0.5 N, 200 μL) was added to the reaction mixture and heated at 110 °C for 20 min. The reaction mixture was cooled to room temperature and was generally diluted with water to a total volume of 2 mL before injecting to the HPLC for purification. A radioactive fraction corresponding the pure [^{18}F]fluororasagiline (t_R = 15–17 min) was collected and diluted with water (50 mL, 18 MΩ). The resulting mixture was loaded on to a pre-conditioned SepPak tC18 plus cartridge. The cartridge was washed with water (10 mL) and the isolated product, [^{18}F]fluororasagiline, was eluted with 1 mL of ethanol in to a sterile vial containing phosphate buffer saline solution (PBS, 9 mL) to give the product in an isolated yield 40–70% corrected for decay, within 75–80 min and a purity of >99%.

4.6. Quality control

The radiochemical purity, identity and stability of [^{18}F]fluororasagiline was determined by analytical HPLC using mobile phase CH_3CN/10 mM H_3PO_4 (15/85) and flow rate of 2 mL/min. The effluent was monitored with an UV absorbance detector (λ = 214 nm) coupled to a radioactive detector (β-flow, Beckman, Fullerton, CA). The retention time (t_R) of [^{18}F]fluororasagiline was 5–6 min. The identity of [^{18}F]fluororasagiline was confirmed by co-injection with the authentic non-radioactive fluororasagiline.

4.7. Specific radioactivity (SA) determination

The SA of the product was measured by analytical HPLC using mobile phase CH_3CN/50 mM H_3PO_4 (15/85) at flow rate of 2 mL/min. SA was calibrated for UV absorbance (λ = 214 nm) response per mass of ligand and calculated as the radioactivity of the radioligand (GBq) divided by the amount of the associated carrier substance (μmol). Each sample was analyzed three times and compared to a reference standard also analyzed three times.

4.8. Determination of MAO inhibition

Human recombinant MAO-B and MAO-A enzymes prepared from insect cells were purchased from Sigma. Kynuramine hydrobromide (Sigma) was used as substrate for the enzymes. The assays were designed to determine the generation of 4-OH-quinoline from kynuramine in the presence of the compounds of interest according to Mahmood et al.[18] A calibration curve of 4-OH quinoline (Sigma) was determined at λ_{Ex} = 310 nm/λ_{Em} = 400 nm and used for calculation of the enzyme activity at the respective compound concentration. This relation was plotted and the IC_{50} determined using the software GraFit 5 (version 5.0.6). The assays were performed as follows. The compounds were diluted 1:2 in each step in 50 mM phosphate buffer (pH 7.4) so that a concentration curve between 0.98 and 2000 nM was generated to determine the IC_{50} for MAO-B and between 0.24 and 50,000 nM for determination of inhibition of MAO-A, respectively. Kynuramine hydrobromide at a concentration of 30 μM was used for both enzymes. For MAO-B 2 μg/mL and for MAO-A 15 μg/mL of the enzyme preparation were added. The reaction was stopped after 20 min incubation at 37 °C and measured at λ_{Ex} = 310 nm/λ_{Em} = 400 nm. IC_{50} values were determined for the respective ligands using the software GraFit 5 (Robin J. Leatherbarrow, version 5.0.6). As internal standards for MAO-B, pargyline, L-deprenyl and rasagiline, and for MAO-A clorgyline were used.

4.9. In vitro autoradiography

Human brains without pathology were obtained from the Department of Forensic and Insurance Medicine, Semmelweis University, Budapest. The brains had been removed during forensic autopsy (control brains) and were handled in a manner similar to that described previously.[19–21] In the present case the post mortem time was 11 h until which the cadaver was stored at ±0 °C. After the removal of the brain it was kept at −85 °C until sectioning after which the whole hemisphere brain slices were kept at −25 °C until the autoradiographic procedures. Ethical permissions were obtained from the relevant Research Ethics Committee of the respective institutions. The sectioning of the brains and the autoradiography experiments were performed at the Department of Neuroscience, Karolinska Institutet. The sectioning took place on a Leica cryomacrocut system. The resulting slices were horizontal brain slices of 100 μm thickness.

The autoradiographic procedures were basically identical with those used by us in former studies.[16,22] Briefly, 100 μm thick whole hemisphere sections were incubated for 90 min at room temperature with 4 MBq/200 mL of the corresponding radiotracer in 50 mM TRIS buffer pH 7.4 containing sodium chloride (120 mM), potassium chloride (5 mM), calcium chloride (2 mM) and albumin (0.1% w/v). After the incubation, the sections were washed in the same buffer three times for five minutes each time at room temperature, briefly dipped in ice cold distilled water, dried and exposed to phosphorimaging plates. The readings were made in a Fujifilm BAS-5000 phosphorimager. Standards were prepared by serial dilution of the radioligand stock solution in assay buffer, using the phosphorimager's Multi Gauge 3.2 image analysis software (Fujifilm). Blocking experiments were performed with 10 μM L-deprenyl, rasagiline and pirlindol, respectively.

4.10. PET measurements in a cynomolgus monkey

One cynomolgus monkey (*Macaca fascicularis*) (6.3 kg) was supplied by the Astrid Fagraeus Laboratory of the Swedish Institute for Infectious Disease Control (SMI), Solna, Sweden. The study was approved by the Animal Ethics Committee of the Swedish Animal Welfare Agency and was performed according to 'Guidelines for planning, conducting and documenting experimental research' (Dnr 4820/06-600) of the KI as well as the 'Guide for the Care and Use of Laboratory Animals'.[23] Anaesthesia was induced by repeated intramuscular injections of a mixture of ketamine hydrochloride (3.75 mg/kg/h Ketalar® Pfizer) and xylazine hydrochloride (1.5 mg/kg/h Rompun® Vet., Bayer). A device was used to fix the position of the head of the monkey during the PET experiments.[24] Body temperature was maintained by Bair Hugger-Model 505 (Arizant Health Care Inc., MN, USA) and monitored by an oral thermometer. ECG, heart rate, respiratory rate and oxygen saturation were continuously monitored throughout the experiments and blood pressure was monitored every 15 min.

The PET measurement was performed using the high resolution research tomograph (HRRT) (Siemens Molecular Imaging). List-mode data were reconstructed using the ordinary Poisson-3D-ordered subset expectation maximization (OP-3D-OSEM) algorithm, with 10 iterations and 16 subsets including modeling of the point spread function (PSF). The corresponding in-plane resolution with OP-3D-OSEM PSF was 1.5 mm full width at half-maximum (FWHM) in the centre of the field of view (FOV) and 2.4 mm at 10-cm off-centre directions.[25] A transmission scan of 6 min using

a single ^{137}Cs source was performed immediately before the injection of the radioligand. List-mode data were acquired continuously for 120 min immediately after intravenous injection of [^{18}F]fluororasagiline. Images were reconstructed with a series of frames 9×20, 3×60, 5×180, 17×360 s for both radioligands. Brain magnetic resonance imaging was performed in a 1.5-T GE Signa system (General Electric, Milwaukee, WI, USA). A T1 weighted image was obtained for coregistration with PET and delineation of anatomic brain regions. The T1 sequence was a 3D spoiled gradient recalled (SPGR) protocol with the following settings: repetition time (TR) 21 ms, flip angle 35°; FOV 12.8; matrix $256 \times 256 \times 128$; 128×1.0 mm slices; 2 NEX. The sequence was optimized for trade-off between a minimum of scanning time and a maximum of spatial resolution and contrast between gray and white matter.

Before delineation of regions of interests (ROIs), the orientation of the brain was spatially normalized by having the high-resolution T1-weighted magnetic resonance images reoriented according to the line defined by the anterior and posterior commissures being parallel to the horizontal plane and the interhemispheric plane being parallel to the sagittal plane. The T1-weighted MR images were then resliced to the resolution of the HRRT PET system, $1.219 \times 1.219 \times 1.219$ mm. The standardized T1-weighted MR images were used as an individual anatomical template for the monkey.

The monkey underwent one study with an iv injection of 163 MBq [^{18}F]fluororasagiline. Regions of interest (ROIs) (the whole brain, the striatum, thalamus, cortex and cerebellum) were delineated on the realigned PET image with the reference to the co-registered MRI.

4.11. Metabolite analysis

A reverse phase HPLC method was used for determination of the percentages of radioactivity corresponding to unchanged radioligand and radiometabolites during the course of a PET measurement.[26] Venous blood samples (2 mL) were obtained from the monkey at 4, 15, 30, 45, 60, and 75 min after injection of [^{18}F]fluororasagiline. Plasma (0.5 mL) obtained after centrifugation of blood at 2000*g* for 2 min was mixed with acetonitrile (0.7 mL). The supernatant acetonitrile-plasma mixture (1.1 mL) and the precipitate obtained after centrifugation at 2000 g for 2 min were counted in a NaI well-counter. The well-counter consists of a NaI crystal (Harshaw, diameter: 38×50 mm; diameter of the well: 16 mm; depth: 38 mm). The crystal is housed inside a led shield cylinder with a wall thickness of approx. 5 cm. Furthermore, the crystal is coupled to a high voltage supply, set to 900 V (Canberra, model 3002), an energy discriminator (Canberra, model 818) and a timer and counter (GE&E Ortec, model 871).

The radio-HPLC system used in these experiments consisted of an interface module (D-7000; Hitachi), a L-7100 pump (Hitachi), an injector (model 7125 with a 1.0 mL loop; Rheodyne) equipped with a μ-Bondapak-C18 column and an absorbance detector (L-7400; 254 nm; Hitachi) in series with a radiation detector (Radiomatic 150TR; Packard) equipped with a PET Flow Cell (600 μL cell). Acetonitrile (A) and phosphoric acid (10 mM) (B) were used as the mobile phase at 6.0 mL/min, according to the following program: 0–10.0 min, (A/B) 15:85→65:35 v/v; 10.0–14.0 min, (A/B) 65:35→15:85 v/v; 14.0–5.0 min, (C/D) 15:85 v/v. Radioactive peaks eluting from the column were integrated and their areas expressed as a percentage of the sum of the areas of all detected radioactive peaks (decay-corrected).

To calculate the recovery of radioactivity from the system, an aliquot (2 mL) of the eluate from the HPLC column was measured and divided with the amount of total injected radioanalyte.

Acknowledgments

The authors would like to thank all the members of Karolinska Institutet PET centre for assistance in the PET experiments including special thanks to Gudrun Nylen, Siv Eriksson, Arsalan Amir and Guennadi Jogolev for excellent technical assistance and to Bayer HealthCare AG for their support.

References and notes

1. Lan, N. C.; Chen, C. H.; Shih, J. C. *J. Neurochem.* **1989**, *52*, 1652.
2. Bach, A. W. J.; Lan, N. C.; Bruke, D. J.; Abell, C. W.; Bembenek, M. E.; Kwan, S. W.; Seeburg, P. H.; Shih, J. C. *FASEB J.* **1988**, *2*, A1733.
3. Foley, P.; Gerlach, M.; Youdim, M. B.; Riederer, P. *Parkinsonism Relat. Disord.* **2000**, *6*, 25.
4. Riederer, P.; Lachenmayer, L.; Laux, G. *Curr. Med. Chem.* **2004**, *11*, 2033.
5. Thebault, J. J.; Guillaume, M.; Levy, R. *Pharmacotherapy* **2004**, *24*, 1295.
6. Sterling, J.; Veinberg, A.; Lerner, D.; Goldenberg, W.; Levy, R.; Youdim, M.; Finberg, J. *J. Neural Transm. Suppl.* **1998**, *52*, 301.
7. Santillo, A. F.; Gambini, J. P.; Lannfelt, L.; Langstrom, B.; Ulla-Marja, L.; Kilander, L.; Engler, H. *Eur. J. Nucl. Med. Mol. Imaging* **2011**, *38*, 2202.
8. Bergstrom, M.; Kumlien, E.; Lilja, A.; Tyrefors, N.; Westerberg, G.; Langstrom, B. *Acta Neurol. Scand.* **1998**, *98*, 224.
9. Bernard, S.; Fuseau, C.; Schmid, L.; Milcent, R.; Crouzel, C. *Eur. J. Nucl. Med.* **1996**, *23*, 150.
10. Ishiwata, K.; Ido, T.; Yanai, K.; Kawashima, K.; Miura, Y.; Monma, M.; Watanuki, S.; Takahashi, T.; Iwata, R. *J. Nucl. Med.* **1985**, *26*, 630.
11. Fowler, J. S.; Macgregor, R. R.; Wolf, A. P.; Arnett, C. D.; Dewey, S. L.; Schlyer, D.; Christman, D.; Logan, J.; Smith, M.; Sachs, H.; Aquilonius, S. M.; Bjurling, P.; Halldin, C.; Hartvig, P.; Leenders, K. L.; Lundqvist, H.; Oreland, L.; Stalnacke, C. G.; Langstrom, B. *Science* **1987**, *235*, 481.
12. Hirvonen, J.; Kailajarvi, M.; Haltia, T.; Koskimies, S.; Nagren, K.; Virsu, P.; Oikonen, V.; Sipila, H.; Ruokoniemi, P.; Virtanen, K.; Scheinin, M.; Rinne, J. O. *Clin. Pharmacol. Ther.* **2009**, *85*, 506.
13. Saba, W.; Valette, H.; Peyronneau, M. A.; Bramoulle, Y.; Coulon, C.; Curet, O.; George, P.; Dolle, F.; Bottlaender, M. *Synapse* **2010**, *64*, 61.
14. Plenevaux, A.; Fowler, J. S.; Dewey, S. L.; Wolf, A. P.; Guillaume, M. *Int. J. Rad. Appl. Instrum. A* **1991**, *42*, 121.
15. Mukherjee, J.; Yang, Z. Y.; Lew, R. *Nucl. Med. Biol.* **1999**, *26*, 111.
16. Nag, S.; Lehmann, L.; Heinrich, T.; Thiele, A.; Kettschau, G.; Nakao, R.; Gulyas, B.; Halldin, C. *J. Med. Chem.* **2011**, *54*, 7023.
17. Couty, F.; Durrat, F.; Prim, D. *Tetrahedron Lett.* **2004**, *45*, 3725.
18. Weissbach, H.; Smith, T. E.; Daly, J. W.; Witkop, B.; Udenfriend, S. *J. Biol. Chem.* **1960**, *235*, 1160.
19. Hall, H.; Halldin, C.; Farde, L.; Sedvall, G. *Nucl. Med. Biol.* **1998**, *25*, 715.
20. Schou, M.; Halldin, C.; Pike, V. W.; Mozley, P. D.; Dobson, D.; Innis, R. B.; Farde, L.; Hall, H. *Eur. Neuropsychopharmacol.* **2005**, *15*, 517.
21. Gillberg, P. G.; Jossan, S. S.; Askmark, H.; Aquilonius, S. M. *J. Pharmacol. Methods* **1986**, *15*, 169.
22. Gulyas, B.; Makkai, B.; Kasa, P.; Gulya, K.; Bakota, L.; Varszegi, S.; Beliczai, Z.; Andersson, J.; Csiba, L.; Thiele, A.; Dyrks, T.; Suhara, T.; Suzuki, K.; Higuchi, M.; Halldin, C. *Neurochem. Int.* **2009**, *54*, 28.
23. Clark, J. D.; Gebhart, G. F.; Gonder, J. C.; Keeling, M. E.; Kohn, D. F. *ILAR J.* **1997**, *38*, 41.
24. Karlsson, P.; Farde, L.; Halldin, C.; Swahn, C. G.; Sedvall, G.; Foged, C.; Hansen, K. T.; Skrumsager, B. *Psychopharmacol. (Berl)* **1993**, *113*, 149.
25. Varrone, A.; Sjoholm, N.; Eriksson, L.; Gulyas, B.; Halldin, C.; Farde, L. *Eur. J. Nucl. Med. Mol. Imaging* **2009**, *36*, 1639.
26. Halldin, C. S. C. -G., Farde, L.; Sedvall, G. Kluwer Academic Publishers **1995**, 55.